Extended Abstracts of the 16th (1984 International) Conference on Solid State Devices and Materials, Kobe, 1984, pp. 571-574

New Photoconductive Detector Based on Doping Superlattices with High-Speed Response over a Wide Energy Range

Y. Horikoshi* and K. Ploog

Max-Planck-Institut für Festkörperforschung

D-7000 Stuttgart 80, Federal Republic of Germany

A new low-capacitance photodetector with high sensitivity in the 0.8 - 1.4 µm wavelength range has been developed from reverse-biased GaAs doping superlattices grown by molecular beam epitaxy. The measured photoresponse of the device at energies far below the gap of the host semiconductor is by orders of magnitude larger than expected from the original theory of doping superlattices because of pronounced tail states existing in the highly doped yet semi-insulating material. The low capacitance of the detector implies high-speed response in the entire long-wavelength range.

1. Introduction

The internal transverse space-charge field existing in doping superlattices results in a substantial radiative electron-hole recombination and in a strong exponential tail of the absorption coefficient at photon energies below the gap of the host material, E_g^o /1-3/. The emission and absorption of photons with energy $E_g^{eff} < \hbar\omega < E_g^o$ is thus possible. In addition, the emission energy and the absorption coefficient are tunable by variation of the effective gap, E_g^{eff}. While the tunable low-energy luminescence of doping superlattices deteriorates at 300 K due to thermal population of high-index subbands, the absorption of photons with energy close to E_g^{eff} is not modified at room temperature if the photogenerated electrons and holes are rapidly swept away from the respective bands.

In this paper we present a new photoconductive detector based on reverse-biased GaAs doping superlattices of different design parameters. The sensitivity of this detector at 1.4 µm reaches more than 20% of the E_g^o response at 0.85 µm. This excellent photoresponse is by orders of magnitude larger than expected from the original theory of doping superlattices and is caused by the existence of pronounced tail states in the forbidden gap region of the superlattices. The capacitance of the reverse-biased device depends only on the geometry of the selective electrodes and can thus be kept extremely low. This implies high-speed response of the new detector.

2. Photodetector Operation

The superlattice configuration for the photodetector consists of 20 to 100 thin alternate n- and p-doped GaAs layers and is provided with n^+- and p^+-regions on two edges extending perpendicular to the layers to form the selective electrodes (Fig. 1a). Through these electrodes a reverse bias voltage V_R is applied to all constituent p-n junctions of the superlattice. Operation of the detector can be understood by inspection of Figs. 1 and 2. The periodic modulation of the energy

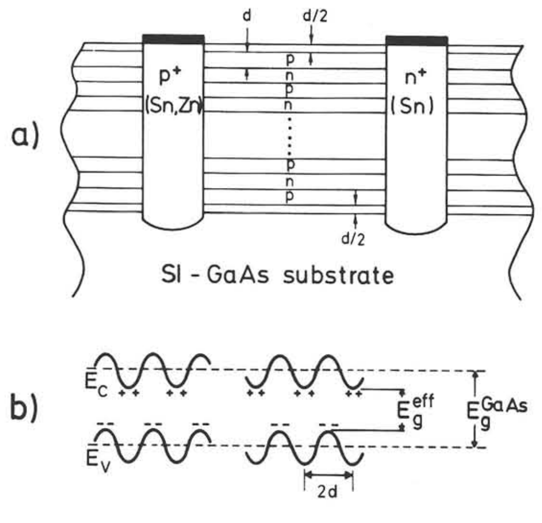

Fig. 1 (a) Layer sequence of GaAs doping superlattice and arrangement of selective n^+- and p^+-electrodes, (b) periodic modulation of real-space energy bands by the positive and negative space charge in the respective layers.

bands by the positive and negative space charge in the respective layers is indicated in Fig. 1b. We have chosen a superlattice configuration where the constituent layers are already totally depleted at zero bias. This requires design parameters providing equal doping densities, i.e. $n_D.d_n = n_A.d_p$, and an effective gap of $0<E_g^{eff}<E_g^o$. In this structure, the intrinsic space-charge field $F_o(x)$ given by the design parameters remains constant upon variation of the reverse bias, because the donors and acceptors within the respective layers are already completely ionized at zero bias. Under these conditions the conduction and valence band edges, E_C and E_V, are flat along the layers, i.e. in x-direction, as shown in Fig. 2a, except for the area close to the n^+- and p^+-contact regions. Because of the total depletion of the layers, the superlattice is highly

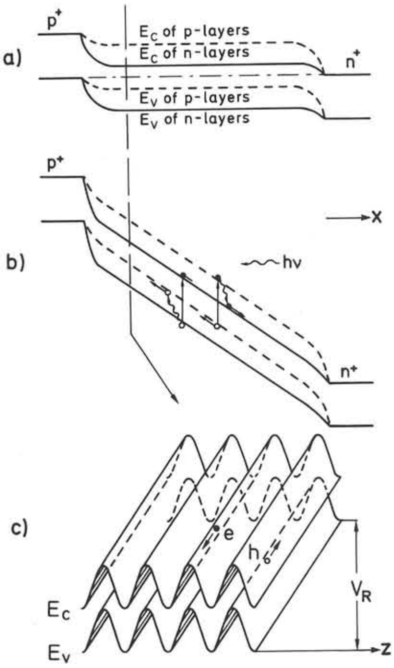

Fig. 2 Schematic real-space energy band diagram of a semi-insulating GaAs doping superlattice with $n_D \cdot d_n = n_A \cdot d_p$ and $0<E_g^{eff}<E_g^o$ provided with selective n^+- and p^+-electrodes; (a) at zero bias in x-direction along the layers viewing the center of each layer type; (b) under operating conditions at high reverse bias with the longitudinal external field tilting the whole structure; (c) vertical section showing the periodic modulation of the energy bands in z-direction and indicating the sweep-out of electrons and holes along the parabolic well channels in the tilted structure.

resistive and behaves like a semi-insulator. Therefore, when a reverse bias is applied via the selective electrodes, a constant longitudinal electric field F_l is added in x-direction parallel to the length of the layers, i.e. the structure is tilted in layer direction, as indicated in Fig.2b and c. Electron-hole pairs generated by the absorption of irradiation are effectively separated in z-direction by the strong space-charge field of the superlattice and then immediately swept away by the longitudinal field in x-direction to the respective electrodes. As a result, recombination of photogenerated carriers is negligibly small and extremely high efficiencies for the absorption process are achieved. Since the photogenerated carriers have relaxation times as short as 10^{-12}s for thermalization in the conduction and valence subband system, the device speed is mainly determined by the time required to sweep out the confined electrons and holes along the parabolic well channels. In addition, due to the rapid sweep-out of the photogenerated carriers by the longitudinal electric field at high reverse bias, the bare space-charge potential of the superlattice experiences only a minor compensation from these excess carriers, and the responsivity of the device for long-wavelength irradiations does not deteriorate during operation.

The sensitivity of our superlattice detector at energies below the gap of the host material is primarily caused by the intrinsic space-charge field, given by $F_o(x) = qNx/\varepsilon$ for $0<x<d/2$ with q= elementary charge, N=doping concentration, and ε= dielectric constant, which enhances the tunnel-

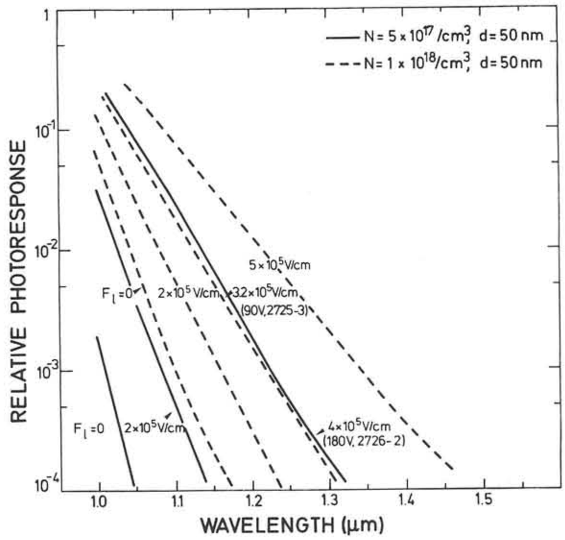

Fig. 3 Relative photoresponse calculated from Eq. (3) for GaAs doping superlattices with design parameters of Table 1 and with various external field strengths F_l.

assisted phototransition between spatially separated electron and hole subbands. The electric field reaches its maximum value of $F_{max} = qNd/2\varepsilon$ at the p-n junction. For the design parameters of our sample # 2726-2 we obtain a maximum internal field of $F_{max} = 2\times10^5$ V/cm at zero bias. When we apply a reverse bias the superimposed longitudinal field F_l can be estimated from the residual free-carrier concentration (see discussion on capacitance) and the applied voltage. With our device we reach $F_l \approx 4\times10^5$ V/cm at V_R=180 V. The total electric field is then given by $F(x)=(F_o(x)^2+F_l^2)^{1/2}$. This electric field applied to a homogeneous semiconductor enhances the absorption coefficient $\alpha(\omega,F)$ at energies below E_g^o due to the Franz-Keldysh effect according to /4,5/

$$\alpha(\omega,F)=\frac{2^{7/3} m_r^{*4/3} |\vec{\varepsilon}\vec{p}_{nn'}|^2 F^{1/3}}{\hbar^{8/3}\, \omega\, m_o^2\, n\, \varepsilon_o\, c} \int_\beta^\infty |A_i(z)|^2 dz \quad (1)$$

where $\beta = (2m_r^*)^{1/3}(E_g-\hbar\omega)/(\hbar qF)^{2/3}$, $\vec{\varepsilon}$ is the radiation polarization vector, $\vec{p}_{nn'}$ is the zero field interband matrix element, m_o is the free and m_r^* the reduced electron mass, n is the refractive index, ε_o is the permittivity of space, c is the velocity of light, and $A_i(z)$ represents the Airy functions. From Eq. (1) we can calculate $\alpha(\omega,F)$ as a function of the electric field by applying the asymptotic form of the Airy functions. Although this calculation is based on the weak-field approximation, the results are still reasonable for absorption coefficients at energies far below E_g^o /4/. Since the total electric field is a function of the position x, we have to average the field-induced absorption coefficient over the superlattice period according to

$$\tilde{\alpha} = \frac{2}{d}\int_0^{d/2} \alpha(\omega,x)\, dx \quad (2)$$

In this way we can obtain the averaged absorption coefficient under the superimposed longitudinal electric field as a function of wavelength. Finally, the photoresponse $J_p(\omega)$ given by the relation

$$J_p(\omega) = qI_o(1-R)\,(1-e^{-\tilde{\alpha}(\omega)\, D}) \quad (3)$$

can easily be calculated when neglecting the spectral dependence of the reflectivity R and using the total thickness of D=2 μm for the doping superlattice (I_o = intensity of incident light).

For GaAs doping superlattices with design parameters of Table 1, detailed results of these calculations are depicted in Fig. 3 for various external field strengths. The photoresponse of the superlattice at energies below the gap of the host material E_g^o is considerably enhanced by both the periodic space-charge field and the superimposed longitudinal field. However, even for the sample with $n_D=n_A=1\times10^{18}cm^{-3}$ and $d_n=d_p=50$ nm the expected sensitivity is not exceedingly high and reaches at 1.3 μm less than 1% of the band edge response when F_l is as high as 5×10^5V/cm. In Sect. 4 we will show that the measured long-wavelength sensitivity is by orders of magnitude larger than those calculated values due to tail states existing in the forbidden gap region of the superlattice.

Table I Design parameters and relative photoresponse of the studied GaAs doping superlattices. V_o is the amplitude of the periodic space charge potential as calculated for total depletion of the respective layers at zero bias /2/ . $2V_o$ is a measure for the reduction of the effective energy gap by the superlattice potential.

sample	$d_n=d_p$ (nm)	$n_D=n_A$ (cm^{-3})	$2V_o$ (eV)
2726-2	50	5×10^{17}	0.45
2725-3	50	1×10^{18}	0.90

3. Experimental

The GaAs doping superlattices formed by alternate Si and Be doping were grown by molecular beam epitaxy (MBE) at 600 °C on semi-insulating (100) GaAs substrates. The superlattice configuration is schematically depicted in Fig. 1a and the design parameters of two representative samples with $n_D=n_A$ and $d_n=d_p$ studied here are given in Table 1. The first GaAs layer following the substrate and the final top layer are always n-type and must have a thickness of d/2 to ensure complete depletion of all constituent n- and p-layers at operating conditions. Rectangular pieces of approximately 1x3 mm^2 area were cleaved from the as-grown wafers. The devices were provided with n^+- and p^+-regions extending perpendicular to the layers on the two far edges by alloying small Sn and Sn/Zn balls, respectively, to form the selective electrodes /3/. A voltage source supplying the reverse bias V_R is connected to the selective n^+- and p^+-electrodes. Chopped monochromatic light from a tungsten iodine lamp passing a grating monochromator was used to irradiate the 1x1 mm^2 detector area. The photocurrent induced by front illumination was measured by a lock-in amplifier.

4. Results and Discussion

The spectral response of the two superlattice detector configurations measured at 300 K in the 0.8 - 1.4 μm wavelength range using a systematically increased reverse bias is shown in Fig. 4. We observe a dramatically increased long-wavelength sensitivity at high reverse bias. The strong transverse electric field given by the design parameters

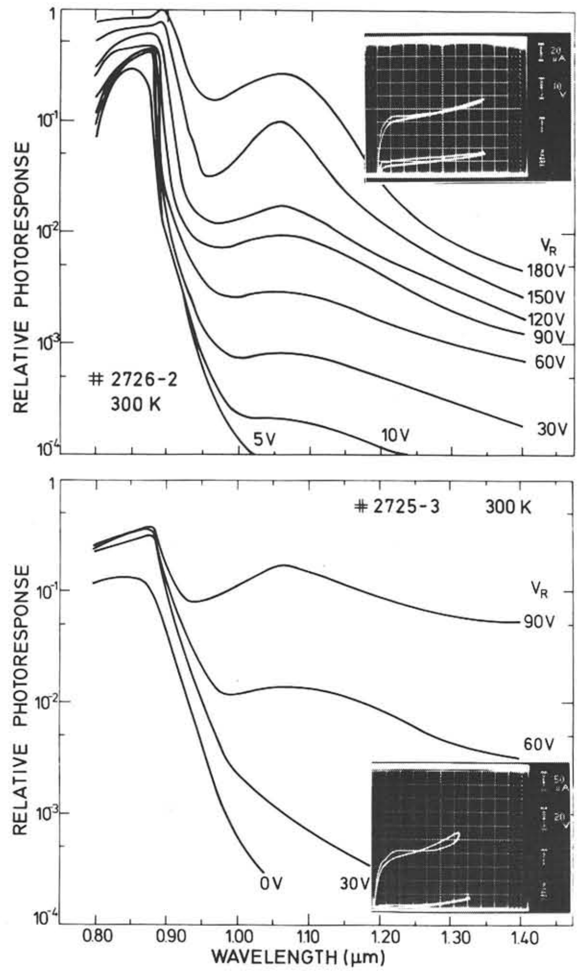

Fig. 4 Spectral photoresponse of reverse-biased GaAs doping superlattices with $d_n=d_p=50$ nm and $n_D=n_A=5\times10^{17}$ cm^{-3} (top) and 1×10^{18} cm^{-3} (bottom). The insets show the reverse I-V characteristics of the devices with and without irradiation.

of the superlattice and enhanced by the longitudinal field due to the external bias allows absorption of long-wavelength irradiation through the Franz-Keldysh effect.

Comparison of calculated photoresponse of Fig. 3 obtained for different longitudinal field strengths with the experimental results of Fig. 4 reveals much higher experimental values than expected from theory, particularly at long wavelength. We interpret this favorable result as follows: Eqs. (1) and (2) are based on the early theoretical approach /2,4/ which was developed for very pure and highly resistive materials where no band tail states are expected (otherwise high electric fields could not have been applied to the sample). The doping superlattices, however, are highly doped - yet highly resistive - and therefore considerable band tail states are expected in the energy gap. Consequently, the probability to find electrons or holes inside the forbidden gap region and the long-wavelength sensitivity is drastically enhanced in the presence of a strong electric field. Our assumption on the existence of tail states for interpretation of the experimental photoresponse data is supported by two additional experimental results. First, the pronounced maximum in the photoresponse spectra around 1.1 μm observed at increased reverse bias may well evidence the existence of a considerably high density of states inside the gap. Second, the influence of tail states on the long-wavelength photoresponse should be more pronounced at higher doping concentrations of the constituent superlattice layers. This effect is indeed observed in the experimental data of Fig. 4 (bottom), which were obtained from sample # 2725-3 with $n_D=n_A=1\times10^{18}$ cm^{-3} yielding an intrinsic electric field of $F_{max}= 3.6\times10^5$ V/cm. Doubling of the doping concentration results in a steep increase of the long-wavelength photoresponse, which at 1.4 µm reaches more than 20% of the E_g^o value at 0.85 µm when applying a reverse bias of $V_R= 90$ V.

The inserts of Fig. 4 show the reverse I-V characteristics with and without irradiation. Although these devices do not show break-down up to V_R = 200 V, we observe a certain dark current. This dark current is strongly reduced immediately after removing the native oxides by etching in HCl, and it increases to the previous value after exposing the device surface to air again. Consequently, optimization of the selective electrodes and appropriate surface passivation is required to minimize the extrinsic contributions to the dark current.

The capacitance of the reverse-biased new detector is only determined by the geometry of the selective electrodes, if the doping superlattice would be perfectly depleted. For the present device, this value would be as low as 10^{-4} pF which implies extremely high-speed response. In practical MBE growth, however, an absolute compensation between donors and acceptors in the respective layers is very difficult, and usually a small amount of residual free electrons (or holes) remains after the complete depletion of p-layers (or n-layers). Thus, the device capacitance depends upon the residual free carrier concentration. For the sample # 2926-2, the capacitance deduced from the residual free carrier concentration is still as low as 0.02 pF, which is much smaller than the measured result of 0.15 pF. This discrepancy may be attributed to the spurious capacitance due to the lead wire and the sample mounting.

5. Conclusion

A new photoconductive detector of low capacitance and with high sensitivity in the 0.8-1.4 µm wavelength range has been fabricated from GaAs doping superlattices grown by molecular beam epitaxy. The highly doped yet semi-insulating superlattice allows application of high reverse bias via selective electrodes also at 300 K. The measured photoresponse of the totally depleted device at energies far below the energy gap of GaAs is by orders of magnitude larger than expected from the original theory of doping superlattices, due to the existence of tail states in the forbidden gap region of the superlattice. Under operating conditions the capacitance of the detector depends only on the electrode geometry and can thus be kept very low. This implies high-speed response of the device. In addition to detector application, this reverse-biased superlattice is attractive for high-speed optical switches with good quantum efficiencies.

Acknowledgement

Part of this work was sponsored by the Bundesministerium für Forschung und Technologie of the Federal Republic of Germany.

References

* on leave from Musashino ECL, NTT, Tokyo 180, Japan

/ 1 / M.I. Ovsyannikov, Y.A. Romanov, V.N.Shabanov, and R.G. Luginova, Sov. Phys. Semicond. 4, 1919 (1971)

/ 2 / G.H. Döhler, Phys. Status Solidi B 52, 79 (1972)

/ 3 / K. Ploog and G.H. Döhler, Adv. Phys. 32, 285 (1983)

/ 4 / J. Callaway, Phys. Rev. 34, A 998 (1964)

/ 5 / G.E. Stillman and C.M. Wolfe, in "Semiconductors and Semimetals", ed. by R.K. Willardson and A.C. Beer (Academic Press, New York, 1977) Vol. 12, p. 291.